The effect of a three-way catalytic converter on particulate matter from a gasoline direct-injection engine during cold-start.

Abstract

This work investigates the effect of a three-way catalytic converter and sampling dilution ratio on nano-scale exhaust particulate matter emissions from a gasoline direct-injection engine during cold-start and warm-up transients. Experimental results are presented from a four cylinder in-line, four stroke, wall-guided direct-injection, turbo-charged and inter-cooled 1.6 l gasoline engine. A fast-response particulate spectrometer for exhaust nano-particle measurement up to 1000 nm was utilised. It was observed that the three-way catalytic converter had a significant effect on particle number density, reducing the total particle number by up to 65 % over the duration of the cold-start test. The greatest change in particle number density occurred for particles less than 23 nm diameter, with reductions of up to 95 % being observed, whilst the number density for particles above 50 nm diameter exhibited a significant increase. The exhaust temperature plays a significant role on the influence of the catalytic converter on the nano-scale particulate matter. It is evident that the dilution ratio of the exhaust sample has a distinct effect on the particulate matter number and size distribution, influencing the engine-out PM more significantly than the tailpipe-out PM during cold-start engine operation. The catalytic converter also has a considerable effect on the estimated total particle mass.

Keywords

Cold-start, gasoline direct-injection, three-way catalytic converter, particulate matter.

1 INTRODUCTION

The main objective of this work is to study the effect of a three-way catalytic converter (TWC) on nano-scale particulate matter (PM) from a gasoline direct-injection (GDI) engine operating under cold-start conditions. A direct comparison between pre-TWC (engine-out) and post-TWC (tailpipe-out) PM emissions will improve our understanding of the effect of a TWC on nano-scale PM, in terms of total particle number concentration, particle size distribution and estimated total particle mass.

PM can be very hazardous to human health. Adverse health effects seem to be linked to nucleation mode (NM) particles, which have equivalent diameters of less than 50 nm, and are the primary particles formed during combustion [1, 2]. These nano-scale particles dominate size distributions in terms of number concentrations and are able to penetrate farther than larger particles into the respiratory system [3, 4]. Recent biological studies suggest that particle surface area and chemistry are more important factors than particle mass [5]. According to Hall *et al*. [6], NM particles may be far more biologically active than accumulation mode (AM) particles of the same chemical composition. The AM is composed of particles which have equivalent diameters ranging from approximately 50 to 1000 nm, and are generally formed via agglomeration of primary NM particles [2]. This suggests that particle surface area or number may be more relevant than particle mass for assessing critical PM levels. Therefore, the cumulative effect of small, nano-scale particles may result in greater toxicity to the lung than a similar mass of larger particles with correspondingly lower surface area [6].

Cold-start emissions are defined as the emissions produced by an engine during the initial warm-up period, after a sufficiently long period of non-use, and before the engine, catalytic converter or other emission reduction systems have reached their optimum operating conditions [7, 8]. Cold-start emissions are known to contribute significantly to emissions

during vehicle drive-cycle testing [9, 10]. There is considerable evidence to support the hypothesis that many short journeys generate considerably more pollution than one journey of the same distance [7]. The short-trip is known to predominate in the driving patterns of a large percentage of the driving population, with a considerable percentage of this consisting of the 'school-trip' [7]. The purpose of a TWC is to convert carbon monoxide (CO), hydrocarbon (HC), and oxides of nitrogen (NO_x) in the exhaust into carbon dioxide (CO_2) and water (H_2O), so that tailpipe-out emissions are at an acceptable level [11]. In other words, the TWC is designed to complete the imperfect combustion process performed by the engine and to bring the exhaust gas mixture to equilibrium composition at relatively low temperatures [7]. However, until the TWC reaches its 'light-off' temperature, the temperature at which conversion efficiency passes 50 %, it remains essentially ineffective [10]. TWCs are not specifically designed to have any effect on combustion generated PM from gasoline engines. Therefore, the effect of the TWC on nano-scale, PM emissions from gasoline engines during cold-start conditions is relatively unknown [12].

A TWC is effective at converting CO, HC and NO_x to CO_2 and H_2O at stoichiometric air-fuel ratios (AFR). At stoichiometric AFR, the exhaust gas should theoretically consist of nitrogen, water and CO_2, with no unconsumed oxygen or fuel remaining [7, 13]. The optimal conversion efficiency for a TWCC lies within a narrow band of AFRs around stoichiometry, known as the 'lambda window' [1]. Gasoline engines fitted with TWCs emit large quantities of CO and HC during the cold-start phase of engine operation as the conversion efficiency is low before the TWC has reached its light-off temperature [9, 12]. Low engine temperatures may increase the likelihood of incomplete vaporisation of the fuel injected into the combustion chamber which can result in a lean vapour-phase mixture, slow burn rate and even misfiring [15]. One approach to reduce some undesirable effects of cold-starting involves injection of excess fuel during the initial warm-up period, with the aim of increasing

engine and exhaust gas temperatures, and reducing the time for the light-off temperature to be reached. However, HC and PM emissions are known to increase dramatically with this strategy [7, 16]. The light-off temperature is a key feature of TWC performance during cold-start, and it has been shown that the time taken to reach light-off temperature is strongly dependent on the rate of temperature increase [10]. The light-off temperature for CO conversion is ~220^{o}C, and the light-off temperature for HC conversion is ~260^{o}C [17].

Several new technologies and approaches have been adopted to reduce the time for the TWC to reach light-off temperature during cold-start. These include two-stage combustion, use of electrically-powered engine block heaters, close-coupling of the TWC to the engine, thermal energy storage devices and secondary injection of air into the exhaust to combat scarcity of oxygen [7, 13, 14]. Close-coupling of the TWC to the engine is the most common approach employed to reduce the time to light-off. However, close-coupling can introduce unwanted heat into the engine compartment and can have detrimental effects on the TWC [18]. This effect is known as thermal aging and can induce other issues such as poisoning (chemical reactions with the catalyst), fouling (deposits blocking the accessibility of the exhaust gas to the catalyst), and loss of wash-coat and other components [19]. These effects can reduce the life of the TWC and increase the time to light-off. Considerable reductions in CO and HC emissions during cold-start have been achieved by using these various technologies to reduce the time for the TWC to reach its light-off temperature. However, the effect of the TWC on PM emissions during transient cold-start engine operation has received little attention.

Significant reduction in PM from diesel engine exhaust is achievable through the use of particle traps. Particle traps are extremely efficient at collecting PM, up to 86% for particles less than 130 nm in diameter [20, 21]. However, this results in a considerable build-up within a few hours of operation [21]. To reduce this build-up or to clean the filter, the

trapped solid-based particles must be oxidised into gaseous CO_2, known as regeneration. Particle trap efficiency and regeneration are primarily dependent on exhaust gas temperature.

2 EXPERIMENTAL SET-UP

Engine - A four cylinder in-line, four stroke, wall-guided direct-injection, turbo-charged and inter-cooled 1.6 l gasoline engine was used in this study. A schematic diagram depicting the experimental set-up is shown in Figure 1, and specifications of the engine are listed in Table A. The engine test bed utilises a Schenck W150 eddy current dynamometer with a CADET V12 engine dynamometer control system, and an AVL advanced combustion analysis system (IndiCom 1.6) for combustion analysis.

Table A: GDI Test Engine Specifications

Bore (mm)	77.0
Stroke (mm)	85.8
Displacement (cm^3)	1598
Compression Ratio	10.5:1
Rated Power (kW)	130 @ 6000 rpm
Maximum BMEP (kPa)	1887 @ 4000 rpm

Particulate Measuring System - The engine test bed system was equipped with a Signal gaseous exhaust emission analyser system along with a Cambustion DMS-500 fast-response particulate spectrometer for exhaust nano-particle measurement. A heated Signal selector switch valve, maintained at 190 ^oC, allowed the user to choose between pre- and post-TWC exhaust samples (i.e. between engine-out and tailpipe-out exhaust samples). The Cambustion DMS-500 provides a number / size spectrum for solid and non-solid particles in the diameter

range between 5-1000 nm [22]. For the purpose of this study the size spectrum was divided into the following five particle size ranges: 5-23 nm, 23-50 nm, 50-100 nm, 100-300 nm and 300-1000 nm diameter, which represent the two main modes of PM, NM (< 50 nm) and AM (> 50 nm). The 5-23 nm size range was investigated based on the recommendations of the European Commission Particle Measurement Programme (PMP) Final Report [23]. A sample of the engine exhaust gases is drawn into the DMS-500 through a 5 m heated line, maintained at 58 ^{o}C along its full length. Within the DMS-500 there are two dilution stages: primary and secondary dilution. The primary dilution factor is kept constant at five, and the secondary dilution factor can be varied from 20 to 500 (a factor of one can also be employed). The dry, pre-heated dilution air is passed through a high efficiency particulate air filter to remove airborne particles. A scroll-type vacuum pump draws the sample through an electrically conductive tube, within which the particles become ionised. A central, high-voltage rod within the classifier column deflects the charged particles toward 22 grounded electrometer rings via electrical repulsion [24]. Particle landing position, and hence size, is a function of its charge and aerodynamic drag.

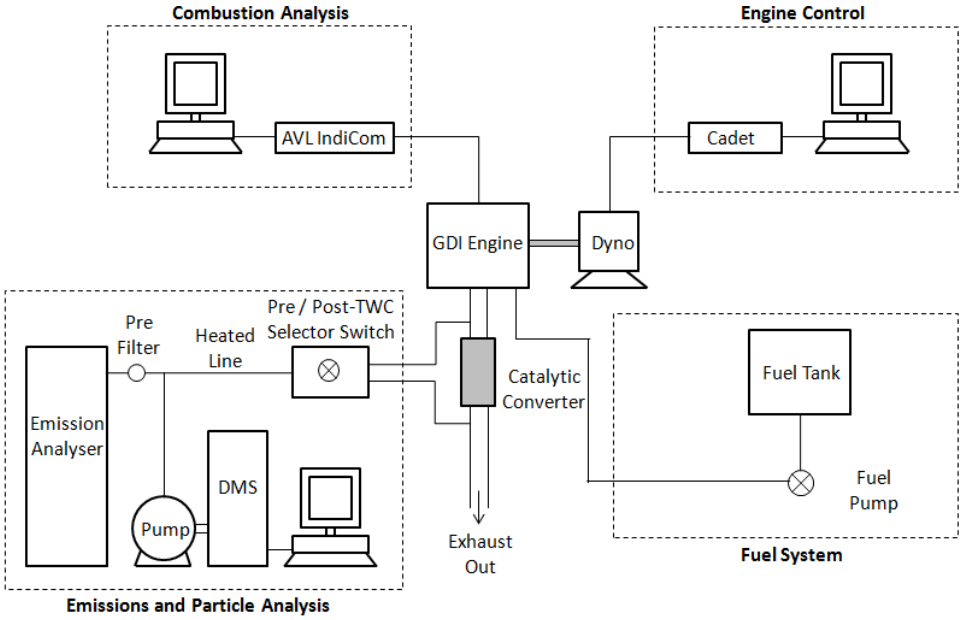

Figure 1: Test cell layout and control systems

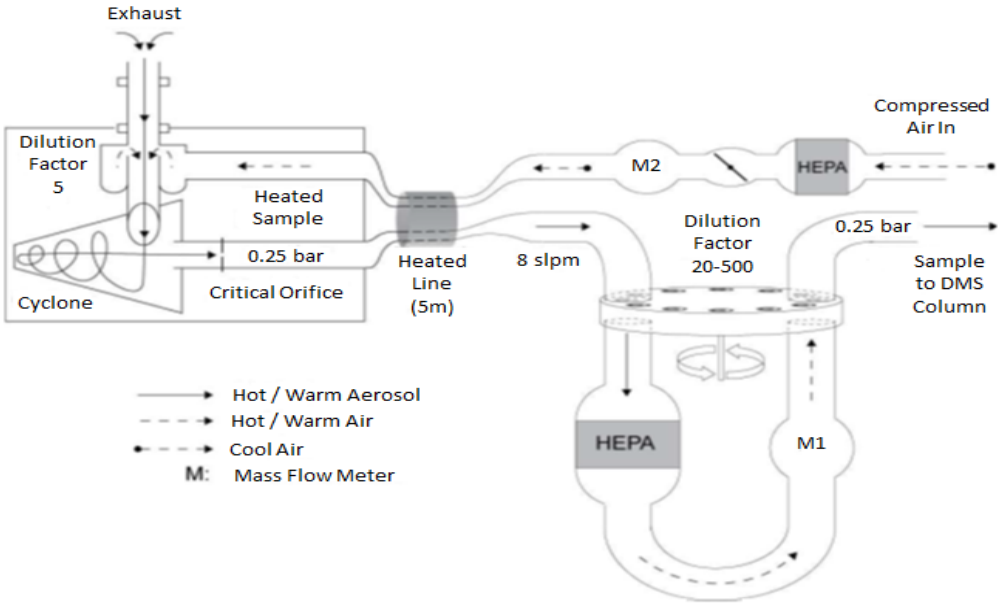

Figure 2: Cambustion DMS-500 dilution system [25]

Fuel - To ensure repeatability of the engine testing, and to eliminate the batch-to-batch variability of pump-grade gasoline, a reference test gasoline was used throughout the test program. The fuel used was a Euro IV certified reference test fuel. Some key specifications of the test fuel are shown in Table B.

Table B: Reference Test Fuel Specifications

Density (kg/litre)	0.75
Research Octane Number	96.5
Volume of Aromatics (%)	31.8
Reid Vapour Pressure (kPa)	57.8
Carbon Content (% mass)	86.01
Hydrogen Content (% mass)	13.09
Oxygen Content (% mass)	0.90

Test method - All experiments were carried out under cold-start conditions. In this study, this involved engine coolant and oil temperatures of 20 ^{o}C prior to engine start-up. The engine was allowed to warm-up at a constant engine speed of 900 rpm (representative of idle conditions after cold-start) and 10 Nm dynamometer load (0.79 bar BMEP, typical of auxiliary loads) to ensure stability and control of the engine operation. The engine warm-up characteristics were controlled by the engine control unit as in a normal engine cold-start procedure. The cold-start test was carried out over a 15 min period, i.e. until the engine coolant temperature had reached ~75 ^{o}C. Pre- and post-TWC tests were performed on separate days to ensure the engine temperature had stabilised overnight to cold-start conditions. All instruments were set to log the data as soon as the engine started to ensure the initial PM emissions were recorded. The CADET V12 and dynamometer system could control the engine speed within ± 2 rpm and the load within ± 1 Nm.

Four exhaust sample dilution ratios (DR) were tested in this study, i.e. total DRs of 5, 100, 125 and 150. A statistical analysis of the repeatability of the PM measurement system was performed over three separate days. Five consecutive tests, each of 3 min duration, were performed at fully warmed up conditions. Tests were performed pre- and post-TWC at a total DR of 100. The Coefficient of Variance (CoV) is used as a measure of repeatability. The CoV of the pre-TWC total particle number density ranged from 3.88 % to 10.80 % over the three days, and the CoV of the post-TWC total particle number density ranged from 2.41 % to 7.83 %, well inside the levels deemed acceptable in the European Commission PMP Final Report [23]. In terms of particle size distributions, the 23-50 nm, 50-100 nm and 100-300 nm size ranges had the lowest CoV; the 5-23 nm and 300-1000 nm had the highest CoV.

3 RESULTS AND DISCUSSION

To study the effect of a TWC on nano-scale PM from a GDI engine operating under cold-start conditions, and to gain an insight into TWC efficiency during cold-start, pre- and post-TWC exhaust emissions were sampled and analysed in terms of particle number density, size distribution, and estimated total mass. Nano-scale PM, measured using the Cambustion DMS-500 fast-response particle spectrometer, in the range of 5-1000 nm equivalent diameter were grouped into five particle size ranges for this investigation: 5-23 nm, 23-50 nm, 50-100 nm, 100-300 nm and 300-1000 nm diameter. Plots showing particle number density use a logarithmic scale due to the large range of values covered by the five particle size ranges. Post-processed, moving-average, data plots for a typical cold-start can be seen in Figure 3. The moving-average plots are based on ten-second time-interval-average data for the duration of the cold-start test, with the main reason for this type of plot being readability and clarity for the reader. All of the following figures show cold-start test results at a total DR of 100, except for Figures 13-15, which shows the effect of DR on pre- and post-TWC particle number density during a cold-start. A single DR was chosen for the comparison of pre- and post-TWC as the effect of the TWC on PM is the main focus of this study. The effect of the TWC on nano-scale PM is characterised by the particle number conversion efficiency (PNCE), which is defined as follows:

$$PNCE\ \% = \frac{Pre{-}TWC\ PM\ No.Density\ -(Post{-}TWC\ PM\ No.Density)}{Pre{-}TWC\ PM\ No.Density} \times 100 \qquad (3.1)$$

For example, in terms of particle number density, positive PNCE indicates a decrease in particle number density after the TWC, and negative PNCE indicates an increase in particle number density after the TWC, for a given size range.

3.1 Particulate Matter Characteristics

Pre- and post-TWC particle number density and exhaust gas temperature, measured during cold-start engine operating conditions, are shown in Figure 3, as a function of time. It is clear from the two PM plots that there is a significant difference between the pre- and post-TWC PM emissions. The steady-state level of the pre-TWC particle number density is ~1.4 x 10^6 N/cc (number/cc). It takes up to 500 s for this steady-state level to be reached. The post-TWC steady-state particle number density level is ~3.2 x 10^5 N/cc, which is reached more rapidly, after ~120 s. From these two plots it can be concluded that, for identical cold-start engine operating conditions, the post-TWC particle number density is considerably lower than the pre-TWC particle number density, and the steady-state level is reached significantly faster for the post-TWC PM than for the pre-TWC PM. This phenomenon holds true for all of the dilution ratios tested, signifying that the PM results are repeatable, and that TWC has a considerable effect on nano-scale PM emissions, regardless of the DR employed.

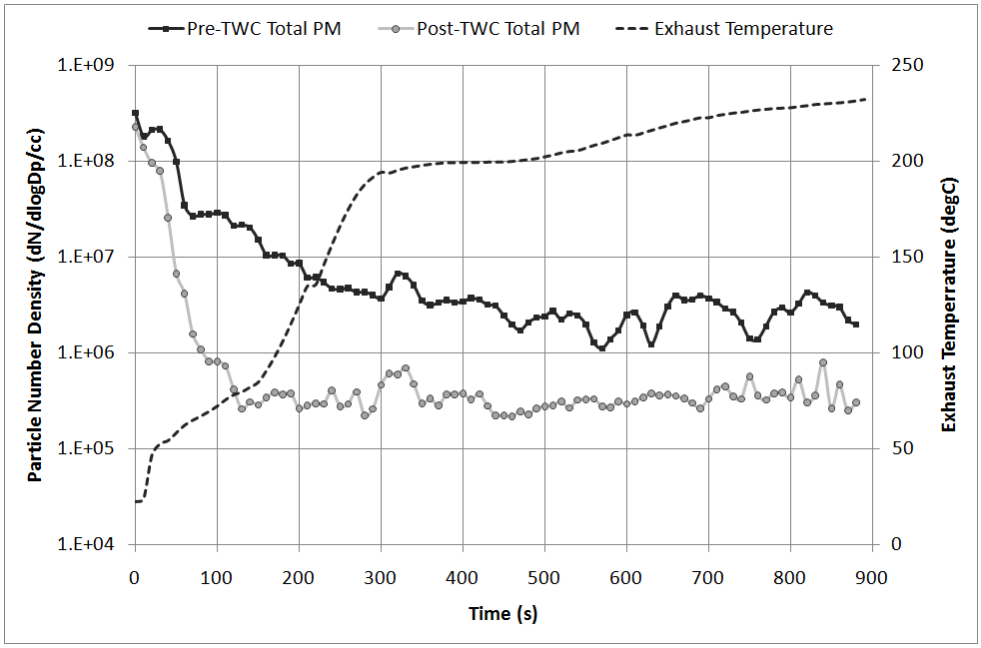

Figure 3: Pre-TWC and post-TWC total particle number density as a function of exhaust temperature, following cold-start from 20 ^{o}C

Figures 4 and 5 show the percentage distribution of particles in each of the five particle size ranges examined in this study, as a function of time over the 15 min cold-start test, for pre- and post-TWC respectively. It is evident that, for pre-TWC exhaust, the 5-23 nm size range dominates throughout the cold-start test, with up to 95 % of particles falling into this size range during the initial stages of the cold-start test. For the post-TWC exhaust, it is apparent that the 5-23 nm size range no longer dominates for the duration of the cold-start test. The percentage distribution of the 5-23 nm size range drops from 73 % to well below 50 %, reaching a minimum of 22 % of the total particle number density. Particles above 23 nm in diameter dominate post-TWC. The percentage distribution of 23-50 nm particles increases from ~8 % pre-TWC to ~22 % post-TWC. Equally, the pre-TWC percentage distribution of the 50-100 nm size range increases from ~1 % to ~28 % post-TWC, with the percentage distribution of the 100-300 nm size range increasing from ~2 % to ~13 % post-TWC. These values indicate that the TWC has the greatest effect on NM particles (5-50 nm size range).

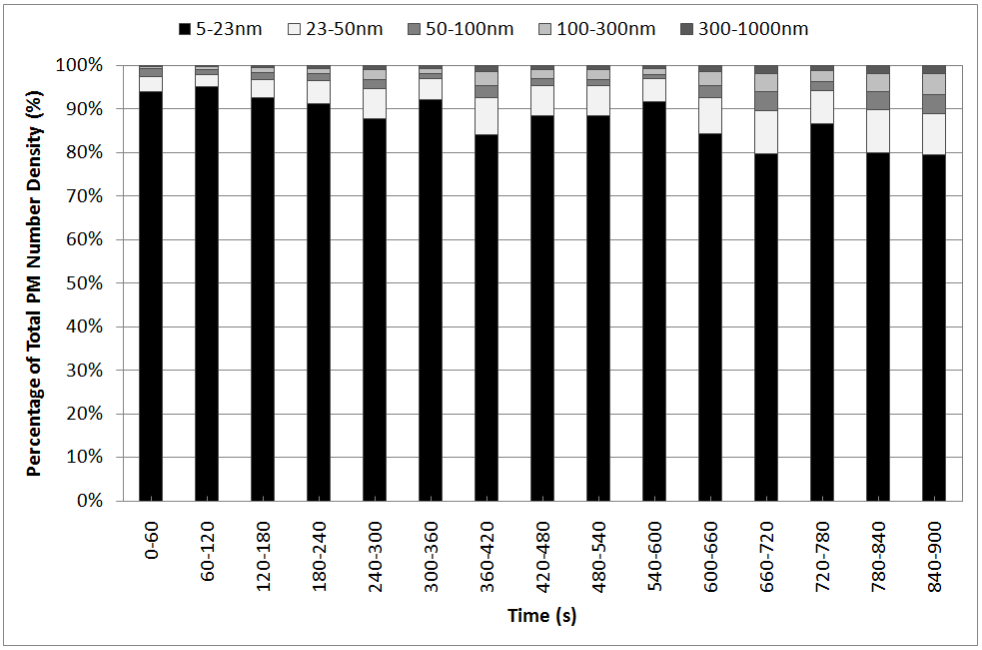

Figure 4: Pre-TWC PM size range percentage of total particle number density as a function of time, following a cold-start from 20 ^{o}C

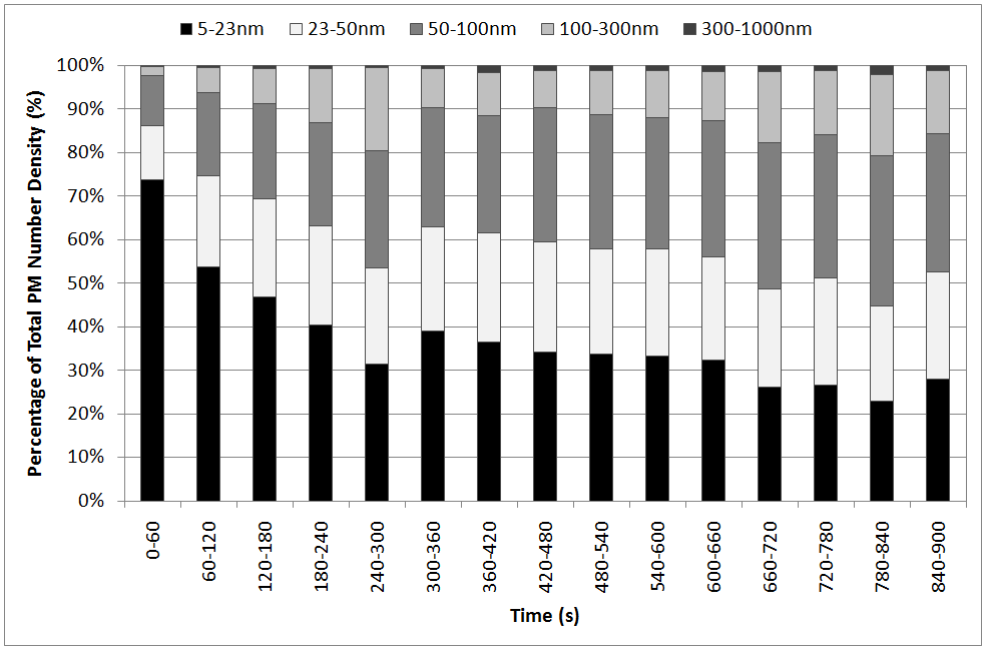

Figure 5: Post-TWC PM size range percentage of total particle number density as a function of time, following a cold-start from 20 ^{o}C

Figures 6 and 7 show the particle number density of each of the five particle size ranges examined in this study, as a function of exhaust temperature over the 15 min cold-start test, for pre- and post-TWC respectively. It is evident from Figure 6 that once the exhaust temperature reaches 180-200 ^{o}C, the pre-TWC particle number density reaches a steady-state level. For the post-TWC PM in Figure 7, the particle number density reaches a steady-state level when the exhaust temperature reaches 80-100 ^{o}C. This indicates that the effective light-off temperature of the TWC for nano-scale PM occurs between 80-100 ^{o}C. This light-off temperature is considerably lower than that for CO and HC, ~220 ^{o}C and ~260 ^{o}C respectively, which shows that the TWC is extremely effective at reducing nano-scale particle number density emissions.

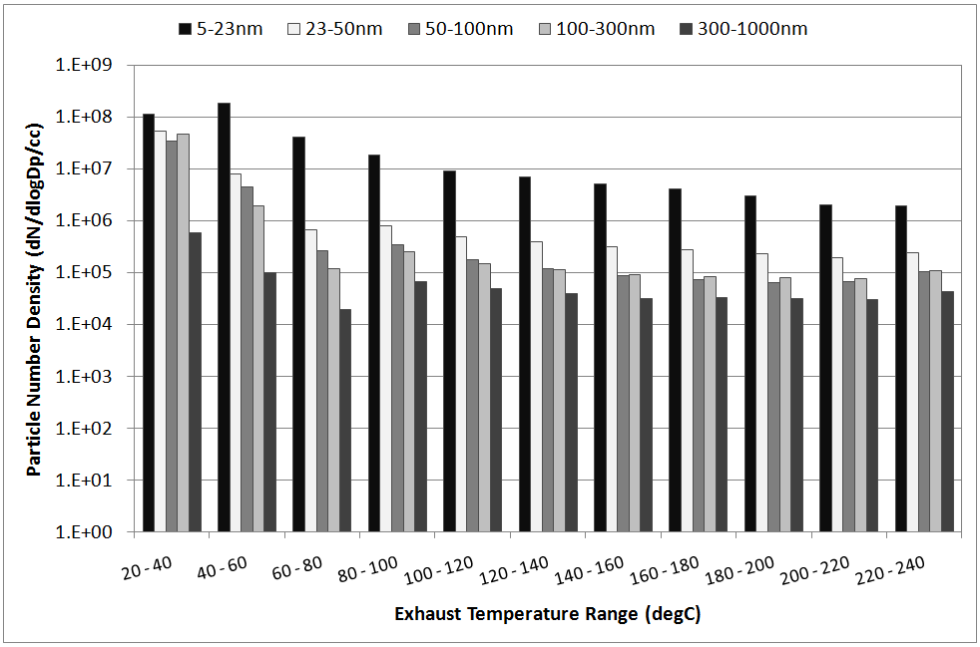

Figure 6: Pre-TWC PM size range number density as a function of exhaust temperature, following a cold-start from 20 ^{o}C

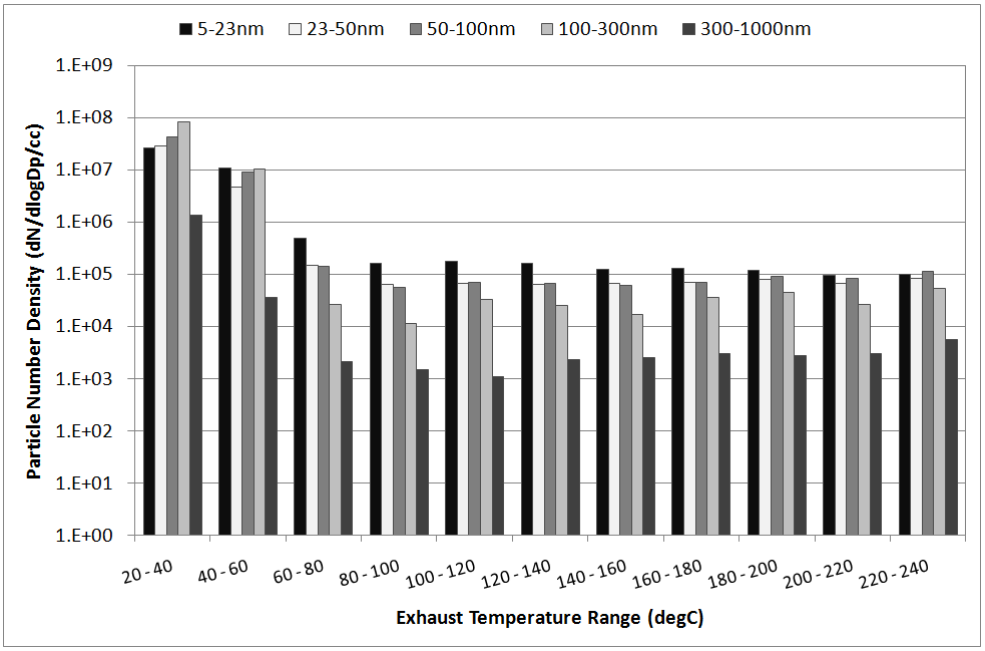

Figure 7: Post-TWC PM size range number density as a function of exhaust temperature, following a cold-start from 20 ^{o}C

Whereas Figures 3 to 7 are shown with respect to time and exhaust temperature for the 15 min cold-start test, Figure 8 shows the total cumulative particle number density for each of the five particle size ranges, averaged over the entire 15 min cold-start test. In terms of the five particle size ranges, Figure 8 shows that both the 5-23 nm and 23-50 nm size range number density is lower post-TWC, and the 50-100 nm, 100-300 nm and 300-1000 nm size range number density is higher post-TWC. These results are in accordance with Figures 4 and 5 which show the shift in dominance from NM particles to AM particles as the exhaust flows through the TWC. It is also evident that the total particle number density is lower post-TWC than pre-TWC. This is due to the large reduction of 5-23 nm and 23-50 nm particles, as seen in Figure 9 which shows the PNCE of the TWC. The PNCE, as stated in Eq. (3.1), is the percentage difference between pre- and post-TWC particle number density.

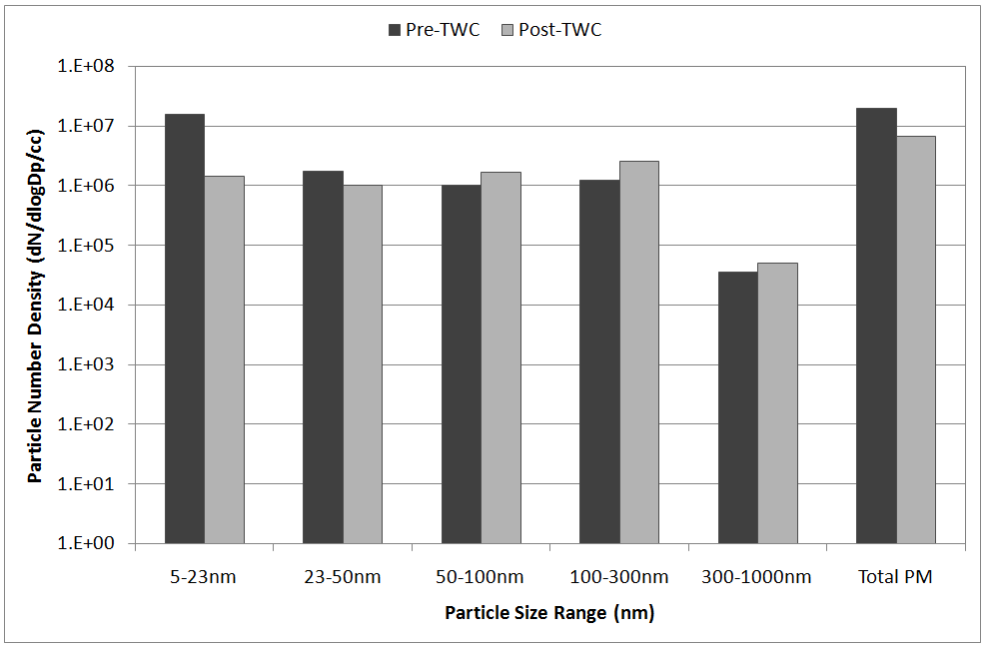

Figure 8: Pre-TWC and post-TWC particle number density, averaged over 15 mins, following a cold-start from 20^{o}C

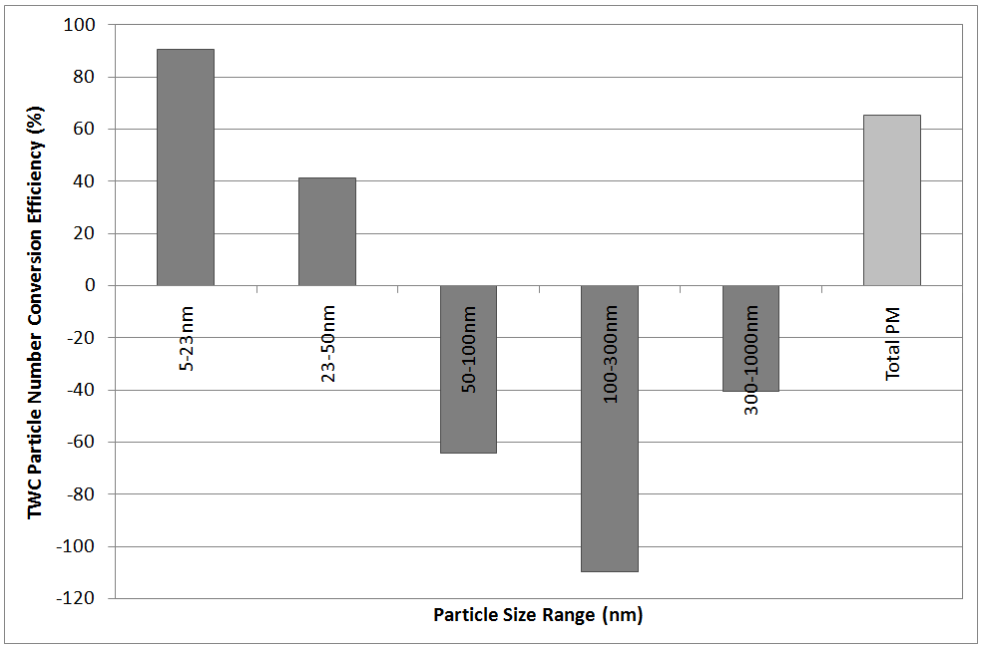

Figure 9: Catalytic converter total and size categorised particle number conversion efficiency in terms of percentage, averaged over 15 mins, following a cold-start from 20^{o}C

Figure 9 indicates that the cumulative number density of the 5-23 nm particle size range is reduced by 90 % post-TWC, with the 23-50 nm size range being reduced by 41 %. It also shows that the cumulative number density of the 50-100 nm, 100-300 nm and 300-1000 nm size ranges all increase post-TWC by 64 %, 109 % and 40 % respectively. This results in an overall reduction in total particle number density post-TWC of 65 %, over the duration of the 15 min cold-start test. This trend of a reduction in NM particles and an increase in AM particles was observed for all DRs tested.

With the shift in the PM size distribution from NM to AM particles post-TWC, the average particle size was found to increase. The geometric mean diameter (GMD) is used as a measure of the equivalent average diameter of the 5-1000 nm particle size range investigated. The GMD of a range of particle diameters is the n^{th} root of the product of n diameters. In Figure 10 it can be seen that the pre-TWC GMD increased from 14.5 nm to 57.9 nm post-TWC, which equates to a 400 % increase in GMD.

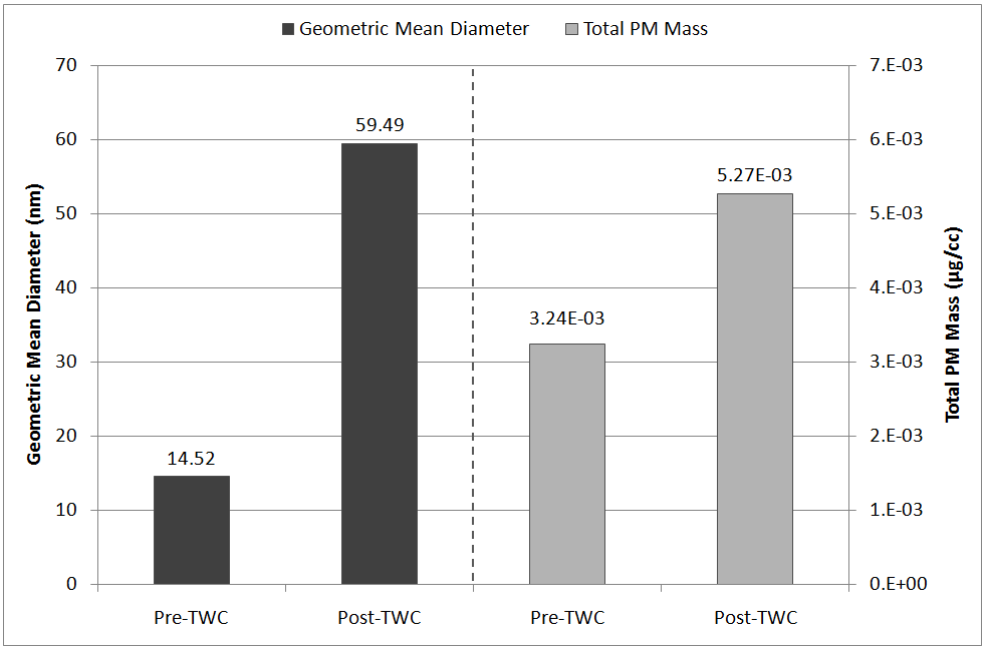

Figure 10: Pre-TWC and post-TWC Geometric Mean Diameter and estimated total PM mass, following a cold-start from 20°C

The estimated total cumulative mass of the pre- and post-TWC PM for the duration of the 15 min cold-start test is shown in Figure 10. The mass is calculated based on Eq. (3.2), drawn for the literature [26]. This equation for mass does not assume that all particles are perfectly spherical, i.e. the mass is not directly proportional to D_p^3, where D_p is particle diameter in nanometers. It assumes that the particles are more fractal like, similar to diesel PM. It does, however, assume uniform density, irrespective of particle size.

$$Mass \ \ \mu g/cc \ = 1.72x10^{-24} \times {D_p}^{2.65} \tag{3.2}$$

It can be seen in Figure 10 that the estimated total PM mass appears to increase post-TWC by ~60 %, even though the total particle number decreases by 65 %. This apparent increase in mass is caused by the shift from NM to AM particles post-TWC. This phenomenon is illustrated further in Figures 11 and 12. Note the logarithmic *x*-axes. Figure 11 shows pre-

TWC particle number and mass distribution with respect to particle diameter for the 15 min cold-start test, with Figure 12 showing post-TWC particle number and mass distribution. To calculate the mass of the PM, Eq. (3.2) is calculated for each individual particle diameter. The number of particles of each individual diameter is than multiplied by the mass of the corresponding particle. The sum of the masses of each particle diameter equates to the total mass of PM. Comparing the particle number distribution pre- and post-TWC, it is clear that there is a significant shift from NM to AM particles. Comparing the PM mass distribution pre- and post-TWC, the peak in mass occurs around the same particle diameter; however post-TWC the mass is considerably higher due to the higher number of AM particles.

This mass is calculated based on particle diameter and particle number density. The assumption of unit density for all particle diameters is questionable. The larger, fractal like, AM particles will have a lower density than the NM particles. Hence this equation will not hold true for all diameters and further work on mass calculation is necessary. Due to equipment restrictions, it was not possible to employ filter-weighing.

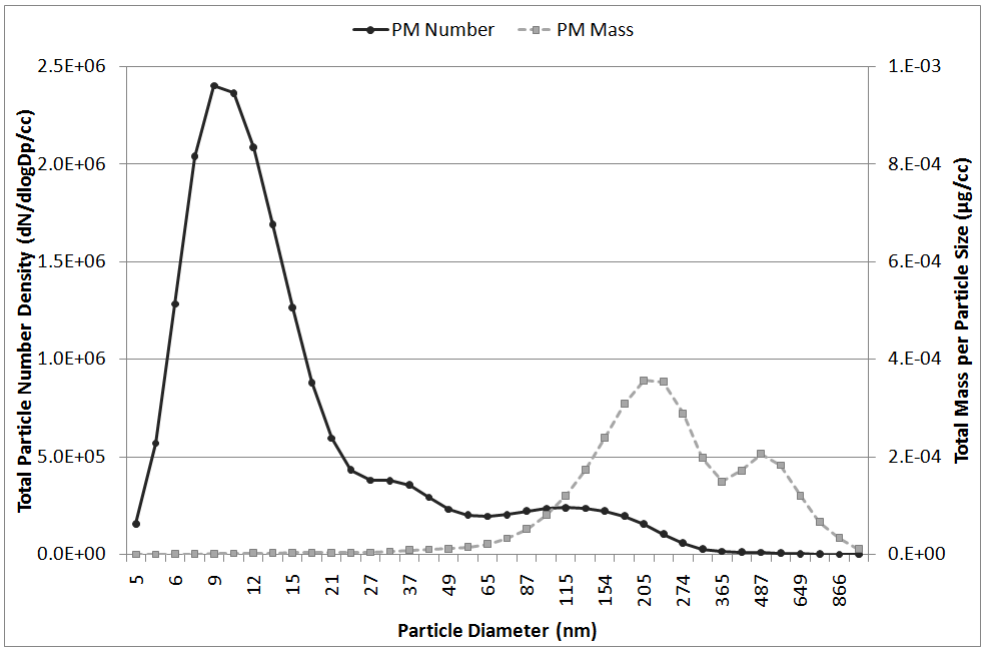

Figure 11: Pre-TWC particle number and mass distribution, following a cold-start from 20^{o}C

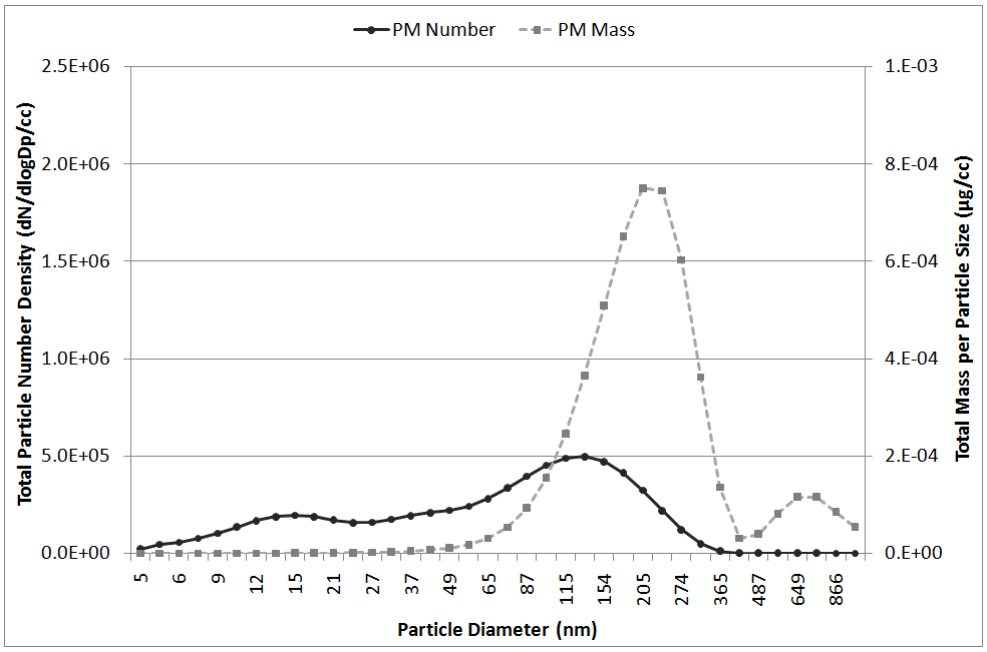

Figure 12: Post-TWC particle number and mass distribution, following a cold-start from 20°C

The reduction in total particle number density and the shift in size distribution from NM to AM particles are thought to be due to coagulation of particles, in combination with possible particle deposition on the catalyst surface and removal of vapour phase volatile particle precursors. The catalyst surface in a TWC is known to be extremely porous, and can act like a particulate filter. In a study carried out by Mizuno *et al*. [27], small pores (20-40 µm in diameter) were shown to trap a significant percentage of PM, reducing the total particle number density, especially NM particles. During the cold-start test, as the exhaust temperature increases toward the light-off temperature for HCs, volatile HC species begin to be oxidised. By removing these HC species, the TWC is removing particle precursors which could have nucleated to form volatile particles before being emitted to the atmosphere. These volatile particles are known to contribute significantly to the number of NM particles as they later re-condense at lower temperatures. Evidence for removal of these volatile particle precursors is strengthened by the observed effects of DR on pre- and post-TWC, discussed in section 3.2. The most obvious mechanism associated with particle number density reduction

in the TWC is coagulation, which may be attributed to the flow patterns within the TWC. The inertia of the PM will carry the PM in a relatively straight line until it impacts upon the wall of the TWC. The passage-ways through the TWC are extremely small in relation to the exhaust manifold and exhaust pipe, hence the tendency for particles to stick together increases. This coagulation could cause many of the NM particles to combine to form larger particles, resulting in the shift from NM to AM particles and also the decrease in particle number density.

Although the individual contribution of each of the three aforementioned mechanisms of particle removal is not precisely known, it is thought that removal of volatile particle precursors in the TWC may have the greatest effect on post-TWC PM.

3.2 Effect of Exhaust Sampling Conditions on Particulate Matter

This section presents the results obtained from the study of exhaust sampling conditions, i.e. dilution ratio, on nano-scale PM measured during cold-start GDI engine operation, for both pre- and post-TWC. It has been recognised by Bouris *et al*. [5] that a large number of AM particles can be formed during sample dilution, by the homogeneous nucleation of volatile species present in the exhaust. The extent of this process can depend on the DR, on the number of carbonaceous particles in the exhaust, and on the surface area available for adsorption or condensation [5].

Figure 13 shows the effect of DR on pre-TWC particle number density for the five particle size ranges investigated during cold-start engine operation, with Figure 14 showing the effect of DR on post-TWC particle number density. In this study a total of four DRs were tested, i.e. total DRs of 5, 100, 125 and 150. These DRs were obtained by varying the secondary dilution factor (1, 20, 25, and 30) while keeping the primary dilution factor constant (5).

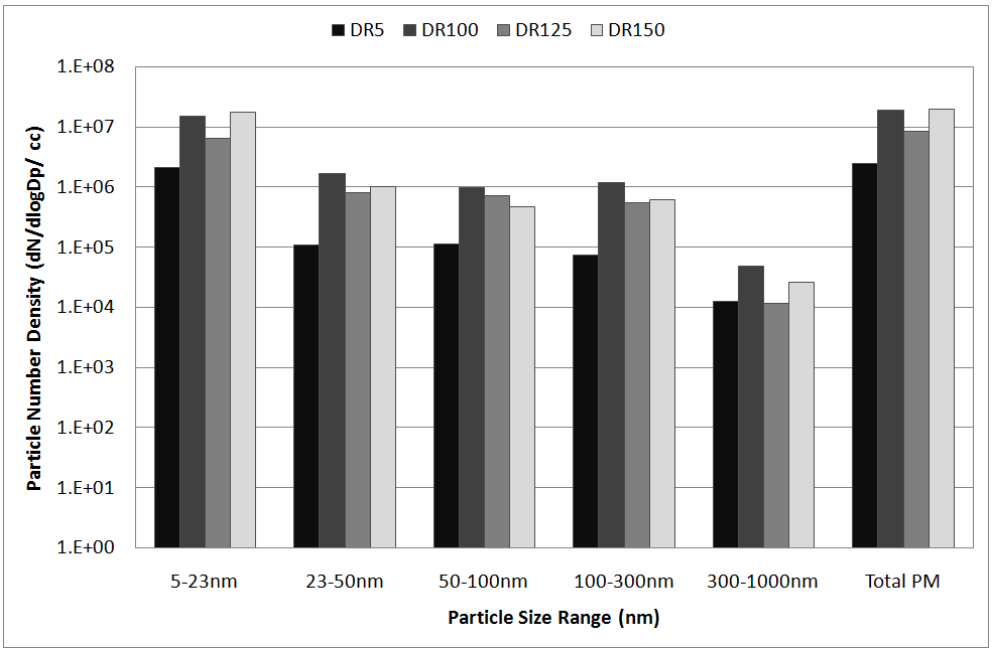

Figure 13: Effect of dilution ratio on pre-TWC total particle number density and PM size ranges, averaged over 15 mins, following a cold-start from 20 ^{o}C

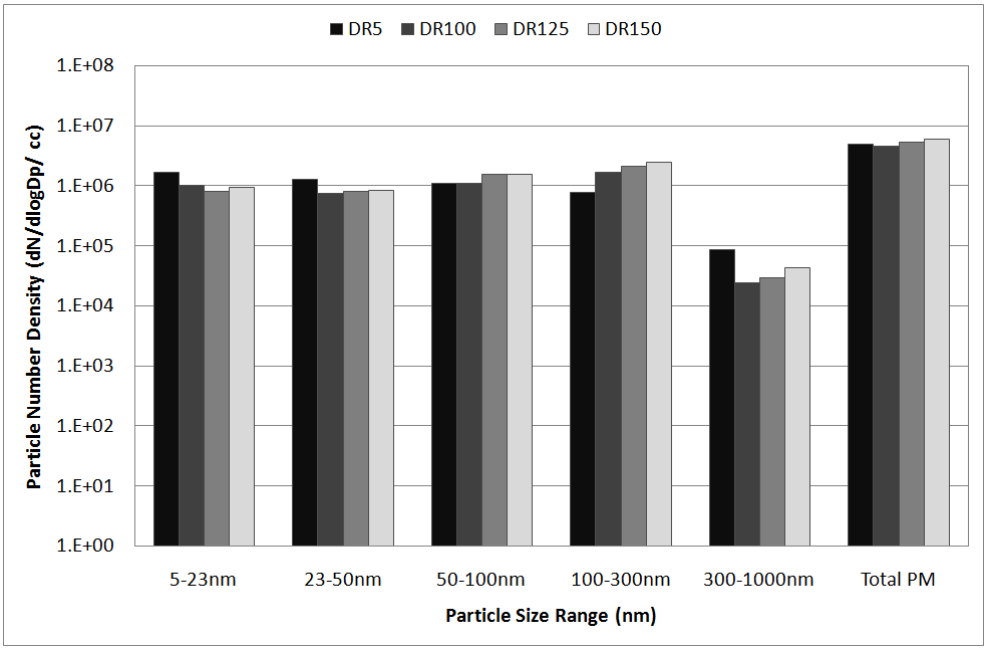

Figure 14: Effect of dilution ratio on post-TWC total particle number density and PM size ranges, averaged over 15 mins, following a cold-start from 20 ^{o}C

From these two figures, it is clear that DR has a greater effect on pre-TWC PM measurement, than on those made post-TWC. This fact can be attributed to the concentration of volatile particles precursors in the pre-TWC exhaust. Increasing the DR pre-TWC results in an increase in total particle number density, but most significantly for the 5-23nm size range. The significant increase in 5-23 nm particle number density as the DR increases can be explained by the effect of dilution on the nucleation rate. According to Giugliano *et al*. [28], the effect of dilution depends on the primary PM concentration and the content of volatile compounds in the exhaust gas. Dilution can prompt the formation of new particles by nucleation of condensable gases. According to Lipsky *et al*. [29], the lower the DR utilised to sample PM, the greater the surface area per unit volume available for condensation of volatile species onto the existing particles. With a larger surface area per unit volume available for condensation, the production of new particles by nucleation of the volatile species is reduced [29]. Hence, a low DR will result in a relatively low concentration of particles. Similarly, utilising a high DR reduces the surface area per unit volume available for condensation of the volatile species onto the existing particles, which can have the effect of increasing the nucleation rate of the volatile species [29]. Hence, a high DR will result in a relatively large concentration of particles, especially in the 5-23 nm size range. For the post-TWC case it can be seen that increasing the DR has very little effect on the total PM, or on the five particle size ranges. This is due to the significantly lower concentration of volatile species in the exhaust gas post-TWC. With a lower concentration of volatile particle precursors, increasing the DR will not cause an increase in the nucleation rate of the volatile species.

Further support for this hypothesis is provided in Figure 15 (a) and (b), which shows the effect of DR on the 5-23 nm particle size range, pre- and post-TWC, for four exhaust temperature ranges. The exhaust temperature ranges were chosen to represent pre-light-off temperature (20-40 ^{o}C), the effective light-off temperature (80-100 ^{o}C), and post-light-off

temperature (120-140 ^{o}C and 180-200 ^{o}C). Two DRs, 5 and 100, were chosen to represent practically undiluted and diluted exhaust, respectively.

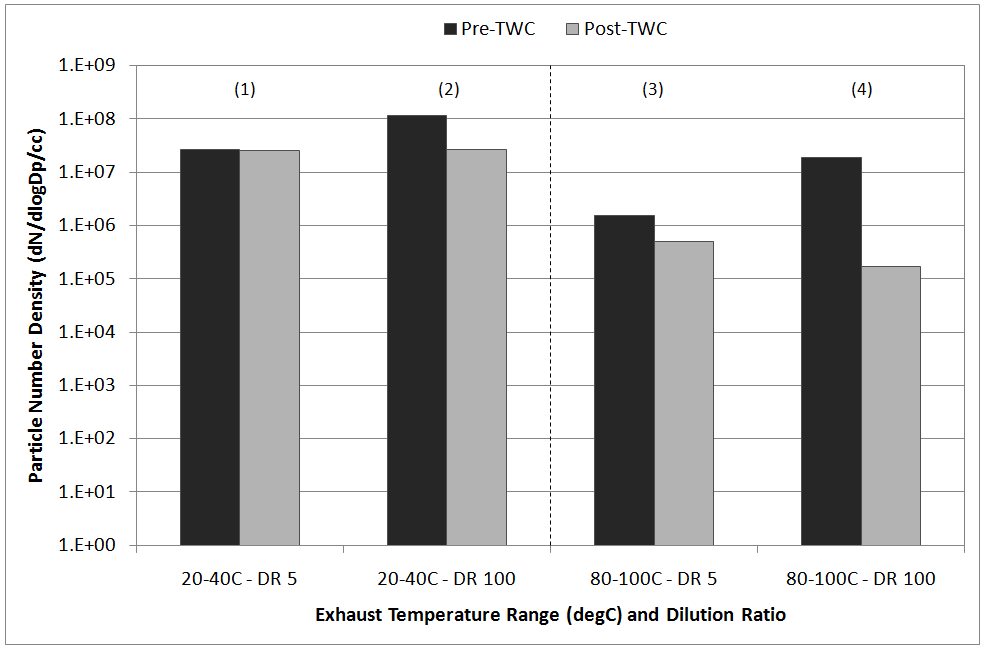

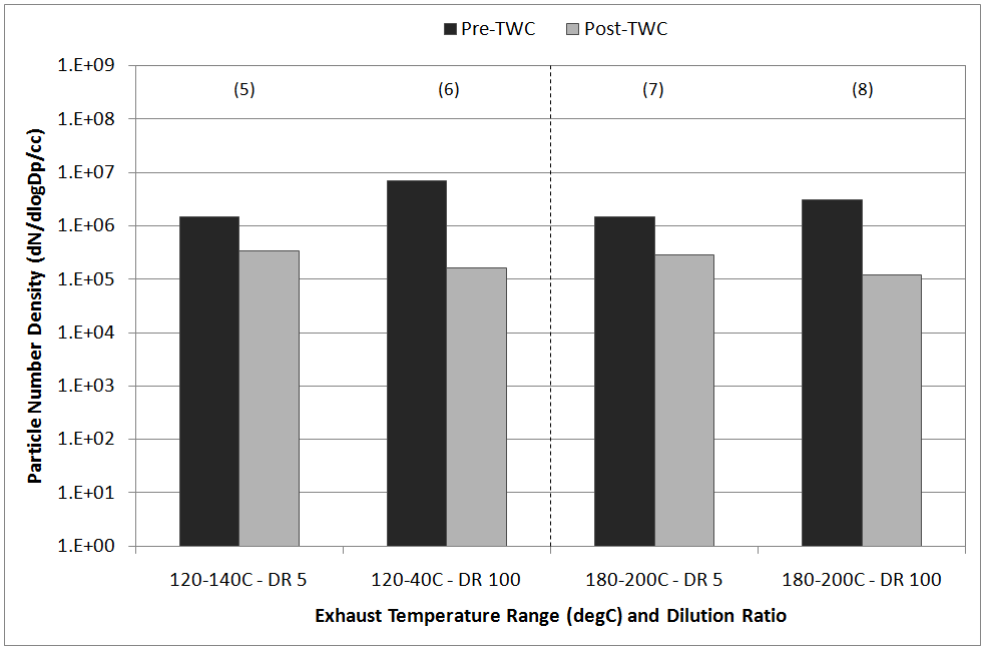

Figure 15 (a) and (b): Effect of DR and exhaust temperature on pre-TWC and post-TWC 5-23 nm particle number density, averaged over 15 mins, following a cold-start from 20 ^{o}C

For the low temperature condition (i.e. pre-light-off temperature) at a DR of 5 (column 1), there is no significant difference between pre- and post-TWC particle number densities. At a DR of 100 (column 2), the effect of increasing DR is far greater pre-TWC due to the high concentration of volatile particle precursors in comparison to post-TWC. In other words, although the TWC has not reached its light-off temperature, the concentration of volatile particle precursors is reduced via deposition and coagulation within the TWC. At the effective light-off temperature at a DR of 5 (column 3), there is now a considerable difference between pre- and post-TWC (i.e. pre-TWC particle concentration is higher). This effect can be attributed to the fact that the TWC has removed a considerable percentage of the volatile particle precursors in the exhaust, which has thus reduced the nucleation rate of new particles upon dilution. At a DR of 100 (column 4), this effect is further enhanced. At this high DR, there are significantly fewer particles post-TWC due to the TWC removing the volatile particle precursors in the exhaust gas. With a lower concentration of volatile particle precursors post-TWC, the nucleation rate of new particles is somewhat reduced. For the high temperature conditions (i.e. post-light-off temperature) at a DR of 5 (columns 5 and 7), the considerable difference between pre- and post-TWC holds true. This trend continues at a DR of 100 (columns 6 and 8).

These results indicate that DR has a different effect on PM measurements, depending on whether the sampling point is upstream or downstream of the TWC. It is also evident that exhaust temperature plays a significant role in understanding the effect of DR on nano-scale PM. This signifies that when sampling pre- and post-TWC PM, different DRs would ideally be utilised in order to accurately study combustion-generated PM. It also shows that a low DR is desirable for cold-start engine testing.

4 CONCLUSIONS

This study investigated the effect of a TWC and sampling dilution on nano-scale exhaust PM emissions from a GDI engine operating under cold-start conditions. From the experimental work carried out, the following conclusions have been drawn:

(1) Post-TWC total particle number density is considerably lower than pre-TWC total particle number density. The particle number density decreases by 65 % across the TWC. The post-TWC steady-state level is reached ~400 s before the pre-TWC steady-state level.

(2) The 5-23 nm size range dominates upstream of the TWC, since it includes up to 95 % of all particles. Post-TWC, the percentage distribution of the 5-23 nm size range drops from ~73 % at the beginning of the cold-start test to a minimum of ~22 % at the end of the 15 min test. The 23-1000 nm size range dominates post-TWC. This implies a shift from NM particles to AM particles.

(3) In terms of particle number conversion efficiency, the TWC reduces the number density of 5-23 nm and 23-50 nm particles by 90 % and 41 % respectively. The number density of 50-100 nm, 100-300 nm and 300-1000 nm particles all increase post-TWC by 64 %, 109 % and 40 % respectively. Based on the study of particle number conversion efficiency with respect to exhaust temperature, the effective light-off temperature of the TWC for PM conversion occurs between 80-100 ^{o}C.

(4) Due to the shift from NM to AM particles, the GMD of the 5-1000 nm size range increases from 14.5 nm to 57.9 nm, an increase of 400 %. With this increase in particle size, the estimated total PM mass appears to increase post-TWC by ~60 %.

(5) The DR utilised in sampling PM has a profound effect on PM measurements made upstream of the TWC, but less of an effect on measurements made post-TWC. Increasing the DR pre-TWC induces an increase in measured particle number density due to nucleation of the volatile particles precursors present in the exhaust gas. Post-TWC, increasing the DR has

very little effect due to the low concentration of volatile particle precursors, as they have been removed by the TWC.

(6) These results imply that when sampling pre- and post-TWC PM, different DRs should be utilised in order to accurately study combustion generated PM. It also shows that a low DR is desirable for cold-start engine testing. Pre-heating the TWC to a temperature above ~200 ^{o}C could lead to a significant reduction in cold-start nano-scale PM.

5 REFERENCES

[1] Kittelson, D.B. Engines and Nanoparticles: A Review. *Journal of Aerosol* Science, 1998, 29(5/6), 575-588.

[2] Graskow, B.R., Kittleson, D.B., Ahmadi, M.R. and Morris, J.E. Exhaust Particulate Emissions from Two Port Fuel Injected Spark Ignition Engines. SAE Technical Paper No. 1999-01-1144, 1999.

[3] Pearson, J.K. Improving Air Quality – Progress and Challenges for the Auto Industry. Pennsylvania, USA: Society of Automotive Engineers; 2001.

[4] D'Anna, A. Combustion-formed nanoparticles. *Proceedings of the Combustion Institute*, 2009, 32, 593-613.

[5] Bouris, D., Crane, R.I., Evans, J.M. and Tippayawong, N. An approach to characterization and after-treatment of particulate emissions from gasoline engines. *International Journal of Engine Research*, 2000, 1, 291-300.

[6] Hall, D.E., King, D.J., Morgan, T.B.D., Baverstock, S.J., Heinze, P. and Simpson, B.J. A Review of Recent Literature Investigating the Measurement of Automotive Particulate: The Relationship with Environmental Aerosol, Air Quality and Health Effects. SAE Technical Paper No. 982602, 1998.

[7] Eastwood, P. Critical Topics in Exhaust Gas Aftertreatment. Hertfordshire, England: Research Studies Press Ltd.; 2000.

[8] Heywood, J.B. Internal Combustion Engine Fundamentals. Boston: McGraw-Hill International Series, Automotive Technology Series; 1988.

[9] Sougawa, Y., Koseki, K., Kawaguchi, H., Nishimura, J., Namiyama, K., Yamagishi, Y. and Ogawa, Y. Improvement of Repeatability in Tailpipe Emissions Measurement with Direct Injection Spark Ignition (DISI) Vehicles. SAE Technical Paper No. 2002-01-2710, 2002.

[10] Shen, H., Shamim, T. and Sengupta, S. An Investigation of Catalytic Converter Performances during Cold-Start. SAE Technical Paper No. 1999-01-3473, 1999.

[11] Samuel, S., Morrey, D., Fowkes, M., Taylor, D.H.C., Gerner, C.P. and Austin, L. Real-world performance of catalytic converters. *IMechE Journal of Automobile Engineering*, 2005, 219(D), 881-888.

[12] Samuel, S., Hassaneen, A.E. and Morrey, D. Particulate Matter Emissions and the Role of Catalytic Converter During Cold Start of GDI Engine. SAE Technical Paper No. 2010-01-2122, 2010.

[13] Tamura, Y., Kituchi, S., Okada, K., Koga, K., Dogahara, T., Nakayama, O. and Ando, H. Development of Advanced Emission-Control Technologies for Gasoline Direct-Injection Engines. SAE Technical Paper No. 2001-01-0254, 2001.

[14] Korin, E., Reshef, R., Tshernichovesky, D. and Sher, E. Improving Cold-Start Functioning of Catalytic Converters by Using Phase-Change Materials. SAE Technical Paper No. 980671, 1998.

[15] Tong, K., Quay, B.D., Zello, J.V. and Santavicca, D.A. Fuel Volatility Effects on Mixture Preparation and Performance in a GDI Engine During Cold Start. SAE Technical Paper No. 2001-01-3650, 2001.

[16] Wiemer, S., Kubach, H. and Spicher, U. Investigations on the Start-Up Process of a DISI Engine. SAE Technical Paper No. 2007-01-4012, 2007.

[17] Hassaneen, A.E. and Lotfy, I. Conversion Efficiency of a 2-Way Catalyst Fitted in a Used Vehicle without Feedback Emission Control System. SAE Technical Paper No. 2005-01-2164, 2005.

[18] Burch, S.D., Potter, T.F., Keyser, M.A., Brady, M.J. and Kenton, F.M. Reducing Cold-Start Emissions by Catalytic Converter Thermal Management. SAE Technical Paper No. 950409, 1995.

[19] Czerwinski, J., Comte, P., Violetti, N., Landri, P., Mayer, A. and Reutimann, F. Catalyst Aging and Effects on Particle Emissions of 2-Stroke Scooters. SAE Technical Paper No. 2008-01-0455, 2008.

[20] Lee, J.W., Jeong, Y.I., Jung, M.W., Cha, K.O., Kwon, S.I., Kim, J.C. and Park, S. Experimental Investigation and Comparison of Nano-Particle Emission Characteristics in Light-Duty Vehicles for Two Different Fuels. *International Journal of Automotive Technology*, 2008, 9(4), 397-403.

[21] Muthaiah, S., Kumar, M.S. and Subramanian, S. CFD Analysis of a Catalytic Converter Using Supported Copper Catalyst to Reduce Particulate Matter and Achieve Limited Back Pressure in Diesel Engine Exhaust. SAE Technical Paper No. 2011-01-1245, 2011.

[22] Cambustion. DMS-500 Fast Particulate Spectrometer User Manual Version 2.0. Available at: http://www.cambustion.com/products/dms500/aerosol [2003-20006, accessed 16 May 2011]

[23] Andersson, J., Giechaskiel, B., Munoz-Bueno, R., Sandbach, E. and Dilara, P. Particle Measurement Programme (PMP): Light-Duty Inter-laboratory Correlation Exercise (ILCELD) Final report (EUR-22775-EN) Rev.1. Available at: http://www.unece.org/trans/main/wp29/wp29wgs/wp29grpe/grpeinf54.html [2007, accessed 20 Sept 2011]

[24] Price, P. and Stone, R. Dynamic Particulate Measurements from a DISI Vehicle: A Comparison of DMS-500, ELPI, CPC and PASS. SAE Technical Paper No. 2006-01-1077, 2006.

[25] Cambustion. DMS-03 Cambustion Application Note - Sampling Engine Exhaust with the DMS500. Available from: http://www.cambustion.com/applications/appinst/DMS500%20%2526amp%3B%20DMS50 [2005-2008, accessed 06 June 2011]

[26] Symonds, J.P.R., Price, P., Williams, P.I. and Stone, R. Density of particles emitted from a gasoline direct injection engine. Cambustion. Available from: http://www.cambustion.com/sites/default/files/downloads/papers/2008/EAC-2008-SYMONDS.pdf, [June 2008, accessed 15 September 2011].

[27] Mizuno, T. and Suzuki, J. Development of a New DPNR Catalyst. SAE Technical Paper No. 2004-01-0578, 2004.

[28] Giugliano, M., Cernuschi, S., Lonati, G., Ozgen, S., Sghirlanzoni, G.A., Tardivo, R., Mascherpa, A. and Migliavacca, G. Ultrafine particles from combustion sources: sampling and measurement. *Chemical Engineering Transactions*, 2008, 16.

[29] Lipsky, E., Stanier, C.O., Pandis, S.N. and Robinson, A.L. Effects of Sampling Conditions on the Size Distribution of Fine Particulate Matter Emitted from a Pilot-Scale Pulverized-Coal Combustor. *Energy & Fuels*, 2002, 16, 302-310.

6 DECLARATION OF CONFLICTING INTERESTS

The authors declare that there is no conflict of interests.

APPENDIX

Notation

TWC	Three-way Catalytic Converter

PM	Particulate Matter
GDI	Gasoline Direct-Injection
NM	Nucleation Mode
AM	Accumulation Mode
CO	Carbon Monoxide
HC	Hydrocarbon
NO_x	Oxides of Nitrogen
CO_2	Carbon Dioxide
H_2O	Water
AFR	Air-fuel Ratio
PMP	Particle Measurement Programme
DR	Dilution Ratio
CoV	Coefficient of Variation
PNCE	Particle Number Conversion Efficiency
GMD	Geometric Mean Diameter